Spatial Diversity and Spatial Correlation Evaluation of Measured Vehicle-to-Vehicle Radio Channels at 5.2 GHZ

Alexander Paier, Thomas Zemen, Christoph Mecklenbrauker, Johan Karedal, Nocolai Czink,
Charlotte Dumard, Fredrik Tufvesson, Andreas Molisch

Abstract

In this contribution, we estimate the spatial diversity order and spatial correlations from channel sounder measurements of doubly-selective vehicle-to-vehicle MIMO radio channels in the 5.2 GHz band. Ivrlac and Nossek [1] have defined a diversity measure of MIMO Rayleigh fading channels which is based on the spatial correlations of the channel. Subsequently, Nabar et al. [2] have shown the existence of an SNR-dependent critical rate for Ricean fading MIMO channels below which reliable transmission with zero outage is achievable. Here, we evaluate and discuss the temporal evolution of the spatial diversity order of doubly-selective vehicle-to-vehicle MIMO radio channels from real-world measurements by extending [1] and [2] to time-variant channels.

SPATIAL DIVERSITY AND SPATIAL CORRELATION EVALUATION OF MEASURED VEHICLE-TO-VEHICLE RADIO CHANNELS AT 5.2 GHZ

Alexander Paier[1], Thomas Zemen[2], Christoph F. Mecklenbräuker[1], Johan Karedal[3],
Nicolai Czink[2,4], Charlotte Dumard[2], Fredrik Tufvesson[3], Andreas F. Molisch[3,5]

[1]Institut für Nachrichtentechnik und Hochfrequenztechnik, Technische Universität Wien, Vienna, Austria
[2]Forschungszentrum Telekommunikation Wien (ftw.), Vienna, Austria
[3]Department of Electrical and Information Technology, Lund University, Lund, Sweden
[4]Smart Antennas Research Group, Information Systems Lab, Stanford University, Stanford, USA
[5]Mitsubishi Electric Research Labs, Cambridge, USA
Contact: `apaier@nt.tuwien.ac.at`

ABSTRACT

In this contribution, we estimate the spatial diversity order and spatial correlations from channel sounder measurements of doubly-selective vehicle-to-vehicle MIMO radio channels in the 5.2 GHz band. Ivrlac and Nossek [1] have defined a diversity measure for MIMO Rayleigh fading channels which is based on the spatial correlations of the channel. Subsequently, Nabar et al. [2] have shown the existence of an SNR-dependent critical rate for Ricean fading MIMO channels below which reliable transmission with zero outage is achievable. Here, we evaluate and discuss the temporal evolution of the spatial diversity order of doubly-selective vehicle-to-vehicle MIMO radio channels from real-world measurements by extending [1] and [2] to time-variant channels.

Index Terms— MIMO channel measurements, V2V channel measurements, spatial correlation, spatial diversity.

1. INTRODUCTION

Current wireless transmission technologies for vehicle-to-vehicle (V2V) communication systems (e.g. 802.11p, WAVE) use single antennas at the transmitter and receiver side only. For safety relevant messages a robust communication link is required. Such a robust communication link can be obtained by exploiting the channels diversity, e.g. spatial diversity by using multiple antennas.
Contributions of the paper: We apply the two different diversity measures introduced in [1] and [2] on real V2V measurement data. Further we characterize the temporal evolution of the spatial diversity in V2V channels and compare the two mentioned diversity measures.
Organization of the paper: In Section 2 we give a short overview about the channel measurement campaign and describe the measurement scenario, which is used for the evaluations in this paper. Section 3 describes the spatial correlation estimation and introduces the diversity measures of Ivrlac and Nabar. Measurement results of the spatial correlation and di-

versity are presented in Section 4 and finally we conclude this paper with Section 5.

2. MEASUREMENTS

2.1. Measurement Description

We carried out the radio channel measurements with the RUSK LUND channel sounder at a center frequency of 5.2 GHz and a measurement bandwidth of 240 MHz. As antenna system we used a 4×4 MIMO circular antenna array with vertically polarized patch antenna elements. The measurement vehicles we used were two similar transporters of the type VW LT35. Tab. 1 presents an overview of the main measurement configuration parameters. With this parameter configuration we were able to measure Doppler frequencies up to 1.6 kHz, which corresponds to a maximum speed of 94 m/s (338 km/h). A detailed description of this radio channel measurement campaign is presented in [3].

2.2. Measurement Scenario

For the evaluation of the diversity measure in this paper we selected one measurement out of a set of 141 measurements that we carried out in and in the vicinity of Lund, Sweden. In this measurement scenario the vehicles are traveling on the highway in opposite directions with a speed of approximately 31 m/s (110 km/h). The measurement has a duration of 10 s. In order to get an overview of this measurement the power-delay profile over time is shown in Fig. 1. We observe a strong line of sight (LOS) path with decreasing delay until the vehicles are passing and increasing delay afterward. In the highway scenario the vehicles are passing after approximately 7 s. Spectral divergence and coherence parameter evaluations for this scenario are presented in [4].

Table 1. Measurement configuration parameters.

| Center frequency, f_c	5.2 GHz
Measurement bandwidth, BW	240 MHz
Delay resolution, $\Delta\tau = 1/BW$	4.2 ns
Frequency spacing, Δf	312.5 kHz
Transmit power, P_{Tx}	27 dBm
Test signal length, τ_{max}	3.2 μs
Number of Tx antenna elements, M_{Tx}	4
Number of Rx antenna elements, M_{Rx}	4
Snapshot time, t_{snap}	102.4 μs
Snapshot repetition rate, t_{rep}	307.2 μs
Number of snapshots in time, N	32500
Number of samples in frequency domain, K	769
Recording time, t_{rec}	10 s
File size, FS	1 GB
Tx antenna height, h_{Tx}	2.4 m
Rx antenna height, h_{Rx}	2.4 m
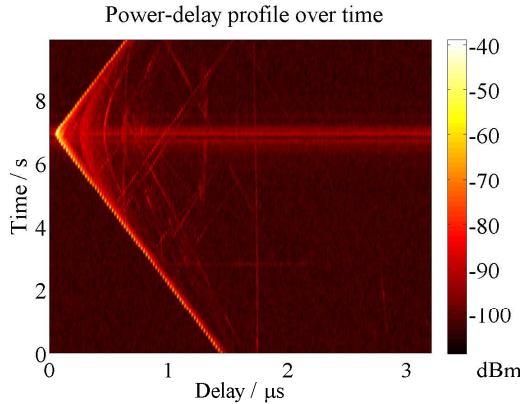
Fig. 1. Power-delay profile over time for Scenario I

3. SPATIAL DIVERSITY AND CORRELATION

The MIMO channel is described by its channel matrix $\mathbf{H}[n,k] \in \mathbb{C}^{M_{Tx} \times M_{Rx}}$ with time index n and frequency index k. We separate the MIMO channel matrix into a mean channel ("Ricean part") and a zero-mean channel ("Rayleigh part").

$$\mathbf{H}[n,k] = \bar{\mathbf{H}}[n,k] + \tilde{\mathbf{H}}[n,k] \tag{1}$$

For statistical characterization, we stack all columns of the channel matrix into one $L = M_{Tx} \cdot M_{Rx}$ dimensional channel vector

$$\mathbf{h}[n,k] = \mathrm{vec}(\mathbf{H}[n,k]) \in \mathbb{C}^{L \times 1}, \tag{2}$$

with Ricean part $\bar{\mathbf{h}}[n,k] = \mathbb{E}\{\mathbf{h}[n,k]\}$.

3.1. Spatial Correlation Estimation

The correlation between the random entries of $\mathbf{H}[n,k]$ can be described by the correlation matrix

$$\mathbf{R}[n,k] = \mathbb{E}\{\mathbf{h}[n,k]\mathbf{h}^H[n,k]\}, \tag{3}$$

where $\mathbb{E}\{.\}$ is the expectation operation and $(.)^H$ represents complex conjugate transpose. The covariance between the channel matrix elements is described in a similar way by the covariance matrix

$$\mathbf{C}[n,k] = \mathbb{E}\{(\mathbf{h}[n,k] - \boldsymbol{\mu}_{\mathbf{h}}[n,k])(\mathbf{h}[n,k] - \boldsymbol{\mu}_{\mathbf{h}}[n,k])^H\}, \tag{4}$$

where $\boldsymbol{\mu}_{\mathbf{h}}[n,k]$ is the mean vector of $\mathbf{h}[n,k]$. In order to get the correlation matrix and the covariance matrix of our measurement data we have to estimate them. The correlation matrix at time n_0

$$\hat{\mathbf{R}}[n_0,k] = \frac{1}{N'} \sum_{n=n_0}^{n_0+N'} \mathbf{h}[n,k]\mathbf{h}^H[n,k] \tag{5}$$

is estimated by averaging over N' time snapshots. The same estimation is used for the covariance matrix

$$\hat{\mathbf{C}}[n_0,k] = \frac{1}{N'} \sum_{n=n_0}^{n_0+N'} (\mathbf{h}[n,k] - \hat{\boldsymbol{\mu}}_{\mathbf{h}}[n_0,k])$$
$$\times (\mathbf{h}[n,k] - \hat{\boldsymbol{\mu}}_{\mathbf{h}}[n_0,k])^H, \tag{6}$$

and the mean vector

$$\hat{\boldsymbol{\mu}}_{\mathbf{h}}[n_0,k] = \frac{1}{N'} \sum_{n=n_0}^{n_0+N'} \mathbf{h}[n,k]. \tag{7}$$

3.2. Diversity Measure (Ivrlac)

This diversity measure (henceforth called Ivrlac diversity measure) is developed in [1]. The Ivrlac diversity measure

$$\Psi_{\mathbf{R}}[n,k] = \left(\frac{\mathrm{tr}(\mathbf{R})}{\|\mathbf{R}\|_F}\right)^2 \tag{8}$$

is defined for frequency flat, Rayleigh fading MIMO channels. It can take values between 1 and L, where 1 means no diversity and L means maximum diversity on the channel. The analysis identifies the eigenvalue spread of $\mathbf{R}$ as the key quantity governing the diversity order of Rayleigh MIMO channels. Since our measured V2V channels show Rician fading behavior we have to modify this diversity measure, in order to make it applicable for our measurement data. For this we evaluate the data without its mean, which results again in a Rayleigh fading channel. This modified diversity measure is based on the covariance matrix

$$\Psi_{\mathbf{C}}[n,k] = \left(\frac{\mathrm{tr}(\mathbf{C})}{\|\mathbf{C}\|_F}\right)^2. \tag{9}$$

As consequence of this, the diversity measure is reflecting the diversity of our MIMO channel without the LOS part.

3.3. Diversity Measure (Nabar)

Nabar et al. distinguish between two different notions of diversity order [2] and discuss the relation between the two quantities. First, they discuss the maximum achievable diversity order d_E over a general MIMO channel with fading. This is the magnitude of the slope of the average error probability for high SNR $\rho \to \infty$ on a log-log scale,

$$d_\mathrm{E} = - \lim_{\rho \to \infty} \frac{\log \overline{P}_e}{\log \rho} = - \lim_{\rho \to \infty} \frac{\rho}{\mathrm{d}\rho} \frac{\mathrm{d}\overline{P}_e}{\overline{P}_e} . \qquad (10)$$

This d_E is achievable by finite code books, e.g. orthogonal space-time block coding (OSTBC) techniques. Alternatively, the diversity order $d_\mathrm{O}(R)$ is defined via the outage probability (packet error ratio) at a given transmission rate R. This leads to the notion of a rate-dependent diversity order

$$d_\mathrm{O}(R) = - \lim_{\rho \to \infty} \frac{\log P_\mathrm{out}(R)}{\log \rho} , \qquad (11)$$

which is relevant for non-finite code books. The corresponding analysis identifies the Hermitian angle $\angle(\mathcal{R}(\bar{\mathbf{h}}), \mathcal{R}(\mathbf{C}))$ between the range of the Rician part $\bar{\mathbf{h}}$ and the range of the covariance matrix $\mathbf{C}$ as a key quantity governing the diversity order of Rician MIMO channels (additionally to the eigenvalue spread of $\mathbf{C}$). Let

$$\delta = \|(\mathbf{I} - \mathbf{Q}\mathbf{Q}^\mathrm{H})\bar{\mathbf{h}}\|^2, \qquad (12)$$

where $\mathbf{Q}$ is an orthonormal basis of the subspace $\mathcal{R}(\mathbf{C})$, then for any fixed transmission rate R, we have

$$d_\mathrm{E} = d_\mathrm{O}(R) = \begin{cases} \infty, & \text{for } \delta > 0, \\ \mathrm{rank}(\mathbf{C}) & \text{for } \delta = 0. \end{cases} \qquad (13)$$

4. MEASUREMENT RESULTS

4.1. Measurement Data Preparation

Before we can use the measured channel matrix $\mathbf{H}[n, k]$ for the calculation of the diversity measures we have to prepare the data, because of the time variance and the existence of noise. As mentioned in Sec. 3.2 and Sec. 3.3 one condition for these diversity measure definitions is a frequency flat channel. In order to fulfill this condition we consider only one frequency bin k out of $K = 769$.

For the estimation of the correlation matrix and covariance matrix, Eq. 5 and Eq. 6, we have to choose the right estimation time. In [5] we found a stationarity time for a similar highway scenario of $23\,\mathrm{ms}$. In order to stay below the stationarity time we choose an estimation time for the highway scenario of $20\,\mathrm{ms}$ ($N' = 64$), which is about 20 wavelengths at a speed of $31\,\mathrm{m/s}$.

Since we observed a strong LOS path in our measurements the Rician and Rayleigh component can be sketched in
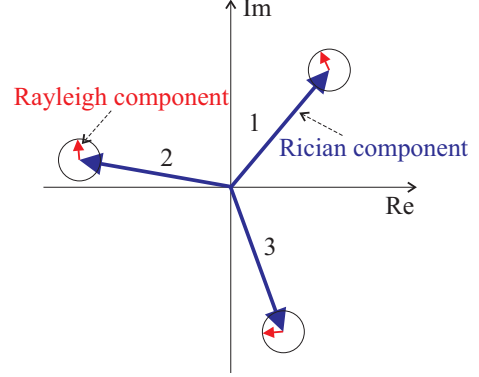

Fig. 2. Rician and Rayleigh component over time

the real-imaginary plane as shown in Fig. 2. The numbers indicate the time index. The phase of the Rician part is changing over time. If we consider the LOS path, the phase is changing linearly over time. In the case of the selected highway scenario there are roughly 3 samples per wavelength, as it is shown in Fig. 2. Since we want to get the Rician component by taking the mean of $\mathbf{h}[n,k]$ over the estimation time, Eq. 7, we have to set the phases of all Rician components equal to the phase of the first component. Otherwise we would average out the Rician component as can be seen easily in Fig. 2.

For this we compare the phase changing with a linear curve and select the one MIMO channel, which shows the minimum mean square error. Then we rotate all MIMO channels back with the linear behavior of this selected channel. Since we shift the phase by a deterministic value, the distribution of the Rayleigh part will not change. These new channel matrix is used for all further evaluations in this paper.

The measurement data is affected by noise. We want to avoid the influence of the noise on the estimation of the diversity measures. For this we choose a threshold based on the signal to noise ratio (SNR), ρ, and apply this on the singular values of the correlation and covariance matrix. In the following we describe this method for the correlation matrix, which is the same method as for the covariance matrix. We calculate the singular value decomposition (SVD) of the correlation matrix $\mathbf{R} = \mathbf{U}\boldsymbol{\Sigma}\mathbf{V}^\mathrm{H}$, where $\boldsymbol{\Sigma}$ is an $L \times L$ matrix with the singular values, σ_l, on the main diagonal. All values smaller than the threshold, which is the maximum singular value divided by the SNR, $\max(\sigma_l)/\rho$, are set to zero. This yields a new singular value matrix $\boldsymbol{\Sigma}'$ and a new correlation matrix $\mathbf{R}' = \mathbf{U}\boldsymbol{\Sigma}'\mathbf{V}^\mathrm{H}$, which is used for the estimation of the diversity measures. For our evaluations we set the SNR to $\rho = 6\,\mathrm{dB}$. Since this is a critical parameter it has to be well choosen, but for this first evaluations, $6\,\mathrm{dB}$ yielded suitable results.

4.2. Correlation Evaluation

In this section we analyze the correlation matrix and the covariance matrix of the highway scenario at time $t = 0\,\text{s}$ and at a frequency of $f = 5.2\,\text{GHz}$. Fig. 3 presents the normalized correlation matrix, where white indicates high correlation and black indicates low correlation. We want to stress the high correlation between the channels 6, 7, 10, 11, 14, and 15. The MIMO channels 6, 7, 10, and 11 are LOS links in the case when the measurement vehicles are approaching, remember that we used circular antenna arrays where the 4 antenna elements were equally distributed over the whole circle. Channel 14 and 15 can be described as "partly" LOS. This was validated by an estimation of the Rician-K-factors with the moment-method of Greenstein et al. [6]. We observed the highest Rician-K-factors from the 4 LOS channels mentioned above, followed by also high Rician-K-factors of the channels 14 and 15.
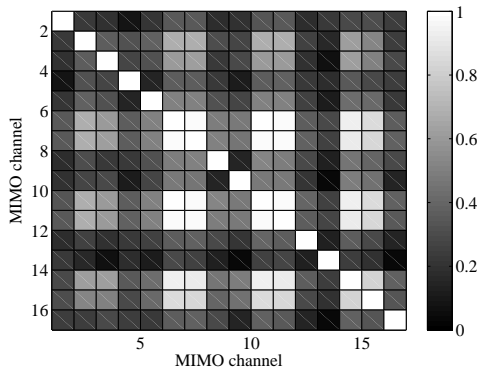

Fig. 3. Normalized correlation matrix of the highway scenario at $t = 0\,\text{s}$ and $f = 5.2\,\text{GHz}$

Fig. 4 shows the normalized covariance matrix for the highway scenario. Since the mean of the channel matrix is subtracted for the estimation of the covariance matrix, the strong LOS paths are not anymore reflected in the covariance matrix. This can be observed in Fig. 4, where there is no strong correlation between the LOS channels mentioned above. The overall correlation between the MIMO channels is much lower compared to the correlation matrix.

4.3. Diversity Evaluation

In this section we compare the two diversity measures of Ivrlac and of Nabar in a selected highway scenario. It has to be mentioned that the Ivrlac diversity measure is valid for frequency flat, Rayleigh fading channels, which is considered by using the covariance matrix for this evaluation. The Nabar diversity measure is valid for frequency flat, Rician fading channels using OSTBCs, or other schemes which turns the MIMO matrix **H** into an effective single-input single-output (SISO) channel as OSTBCs do. Further information about
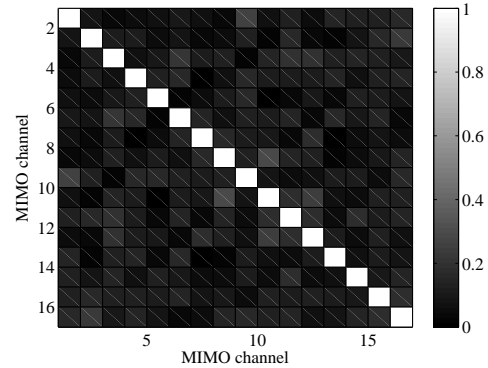

Fig. 4. Normalized covariance matrix of the highway scenario at $t = 0\,\text{s}$ and $f = 5.2\,\text{GHz}$

the conditions of the diversity measures are presented in [1] and [2]. In spite of the different conditions of the two diversity measures, we found similar results, which are presented in the following.

Fig. 5 presents the diversity measures at 4 time snapshots of the 10 s measurement run. The curves in Fig. 5 (a)-(d) were generated by taking the mean over 10 frequency bins for the Ivrlac diversity and the median value over 10 frequency bins for the Nabar diversity. The diversity measure of Ivrlac and Nabar show the same overall behavior, where the Nabar diversity measure is mostly higher. Only at a small diversity, in our example Fig. 5 (c), the Ivrlac diversity is in some cases higher than the Nabar diversity. Note that the Nabar diversity is integer-valued, because it is defined as the rank of the correlation matrix.

Both diversities are varying over the 240 MHz measurement bandwidth. This frequency selectivity is also changing over time. Further we observe a strong distance dependency of the diversity measures. Remember that we consider a highway scenario, where the vehicles are traveling in opposite directions. At time 2.5, Fig. 5 (a), where the distance between the two vehicles is 284 m, we observe a median value of 9 for the Nabar diversity and a mean value of 7.1 for the Ivrlac diversity. At time 5 s, Fig. 5 (b), at a distance of 132 m, a Nabar diversity of 7 and a Ivrlac diversity of 5.6 are observed. In Fig. 5 (c) the vehicles are only 49 m away from each other and the diversity is 2 with the Nabar evaluation and 1.9 with the Ivrlac evaluation. At a time snaphot of 10 s the vehicles have again a larger distance of 197 m, which reflects also in a higher Nabar diversity measure of 11 and a higher Ivrlac diversity measure of 9.4.

5. CONCLUSIONS

In this paper we applied the spatial diversity measures of Nabar [2] and Ivrlac [1] on real V2V channel measurement data, conducted on a highway. We found a high spatial corre-
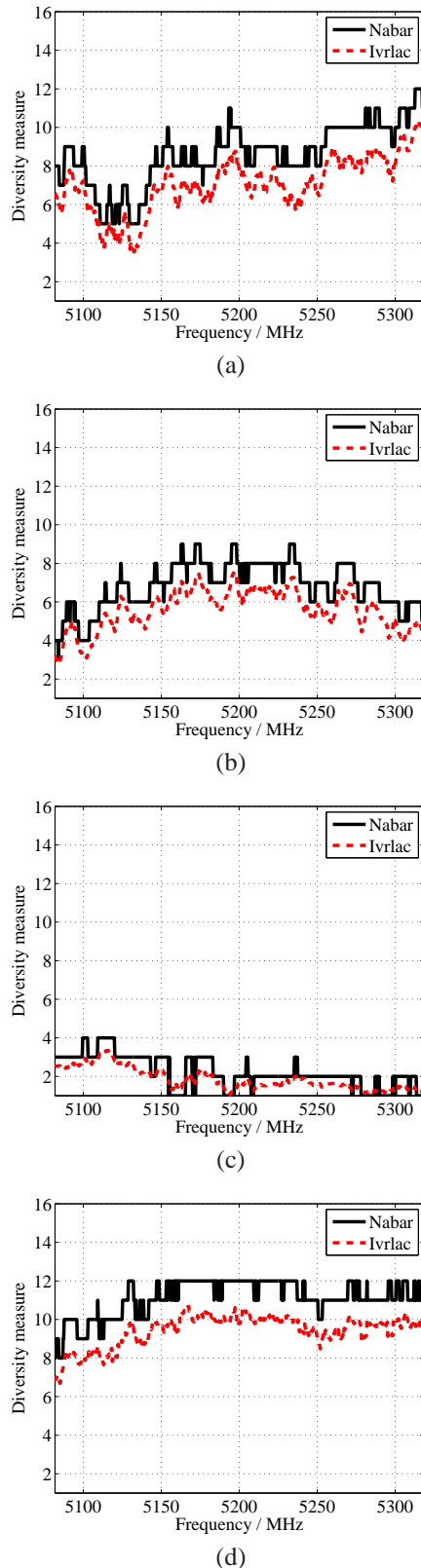
Fig. 5. Diversity of the highway scenario at (a) 2.5 s, (b) 5 s, (c) 7.5 s, and (d) 10 s

lation in line of sight MIMO channels. Further we evaluated the temporal evolution of the spatial diversity, where we found a strong dependency on the distance between the two vehicles. The spatial diversity is much lower, when the vehicles are closer and is roughly inversely proportional to the K-factor of the channel.

6. ACKNOWLEDGMENTS

7. REFERENCES

[1] M. T. Ivrlac and J. A. Nossek, "Quantifying diversity and correlation in Rayleigh fading MIMO communication systems," in *3rd International Symposium on Signal Processing and Information Technology (ISSPIT)*, Dec. 2003, pp. 158–161.

[2] R. U. Nabar, H. Bölcskei, and A. J. Paulraj, "Diversity and outage performance in space-time block coded Ricean MIMO channels," *IEEE Transactions on Wireless Communications*, vol. 4, pp. 2519–2532, Sep. 2005.

[3] A. Paier, J. Karedal, N. Czink, H. Hofstetter, C. Dumard, T. Zemen, F. Tufvesson, C. F. Mecklenbräuker, and A. F. Molisch, "First results from car-to-car and car-to-infrastructure radio channel measurements at 5.2 GHz," in *International Symposium on Personal, Indoor and Mobile Radio Communications (PIMRC 2007)*, 3-7 Sep. 2007, pp. 1–5.

[4] L. Bernadó, T. Zemen, A. Paier, G. Matz, J. Karedal, N. Czink, C. Dumard, F. Tufvesson, M. Hagenauer, A. F. Molisch, and C. F. Mecklenbräuker, "Non-WSSUS vehicular channel characterization at 5.2 GHz - spectral divergence and time-variant coherence parameters," in *XXIXth URSI General Assembly*, 9-16 Aug. 2008.

[5] A. Paier, T. Zemen, L. Bernadó, G. Matz, J. Karedal, N. Czink, C. Dumard, F. Tufvesson, A. F. Molisch, and C. F. Mecklenbräuker, "Non-WSSUS vehicular channel characterization in highway and urban scenarios at 5.2 GHz using the local scattering function," in *International Workshop on Smart Antennas (WSA 2008)*, 26-27 Feb. 2008, pp. 9–15.

[6] L. J. Greenstein, D. G. Michelson, and V. Erceg, "Moment-method estimation of the Ricean K-factor," *IEEE Communications Letters*, vol. 3, pp. 175–176, Jun. 1999.